PAPER

Investigating structural, electronic, magnetic, and optical properties of Zr doped and Ti-Zr co-doped GaN for optoelectronic applications

Physica Scripta

PAPER

Investigating structural, electronic, magnetic, and optical properties of Zr doped and Ti-Zr co-doped GaN for optoelectronic applications

M Junaid Iqbal Khan[1,2,*], Juan Liu[2], Saima Batool[2], Abid Latif[3], Iqra Majeed[2], M Yousaf[2], Imran Taj[2], Hamid Ullah[4], Zartasha Mustansar[5], Masood Yousaf[6], Javed Ahmad[2] and Mazia Asghar[4]

[1] School of Optics and Photonics, Beijing Institute of Technology (BIT), 10081, Republic of China
[2] Laboratory of Theoretical and Experimental Physics, Department of Physics, Bahauddin Zakariya University (60800), Bosan Road, Multan, Pakistan
[3] Department of Civil Engineering, Faculty of Engineering and Technology, Bahauddin Zakariya University (60800), Bosan Road, Multan, Pakistan
[4] Department of Physics, Riphah International University, Lahore Campus, Pakistan
[5] Department of Computational Engineering, Research Center for Modeling and Simulation (RCMS), National University of Science and Technology (NUST), Academics-1 Building, NUST campus, H-12, Islamabad, Pakistan
[6] Department of Physics, Division of Science and Technology, University of Education, Lahore 54770, Pakistan
* Author to whom any correspondence should be addressed.

E-mail: drjunaid.iqbalkhan@bzu.edu.pk

Keywords: gallium nitride (GaN), Zr doping, Ti-Zr co-doping, density of states, optical properties

RECEIVED
21 May 2022

REVISED
16 October 2022

ACCEPTED FOR PUBLICATION
1 December 2022

PUBLISHED
14 December 2022

Abstract

Search of new novel materials for bringing advancement in the field of energy storage and optical materials is tremendously growing in order to meet future challenges. Gallium nitride (GaN) shows exceptional optoelectronic behavior which is highly needed for production of optoelectronic devices. Therefore, in this research study, we investigate the structural, electronic, magnetic, and optical properties of pure GaN, titanium doped GaN (Ti@GaN), zirconium doped GaN (Zr@GaN) and Ti-Zr co-doped GaN using the Wien2k code. Proactive role of dopants Ti and Zr *d*-states is observed which appreciably tune electronic properties. GaN remains non-magnetic after zirconium substitution with Ga atom however, Ti doping and Ti-Zr co-doping produce magnetism into GaN with total magnetic moments of 0.99 μ_B, and 1.503 μ_B, respectively. Substitution of Ti/Zr into GaN may be more favorable at N-rich conditions due to lower formation energy. Absorption spectrum of Ti@GaN and Zr@GaN show blueshift while for Ti-Zr@GaN material exhibit redshift. However, absorption spectra of both proposed materials significantly enhanced in the UV region which propose their potential uses in the high power UV optoelectronics, spintronics, photonics devices and in solid state nano-emitters.

1. Introduction

At present, a great research interest has been found in semiconductor physics due to their applications in optoelectronics, spintronics, photonics, and power electronics. III-nitride semiconductors [1, 2] come forward because of their wide applications in the short wavelength region. Gallium nitride (GaN) belongs to III-nitrides and remains the focus of research in the current decade because of its strong candidacy in the progress of emerging technology. Energy efficiency, higher drift velocities, high chemical stability, better doping efficiencies, and economical cost of GaN emphasize its uses in current research [3, 4]. Moreover, GaN preferred as an ideal material for production of high electron mobility transistors (HEMTs) [5], spin lasers [6], solid state lightning [7], high resolution micro displays [8], UV optoelectronic transistors [9], biological sensors [10], optogenetics [11], light emitting diodes [12], and photonic devices [13]. Physical properties of gallium nitride may be changed upon adding dopants and several studies (experimental and theoretical) may be found in literature which further explores its scope in various applications [14–20]. Knowing this fact, we performed current study in order to explore and manifest the electronic structure, magnetic and optoelectronic properties of GaN with zirconium doping and Zr-Ti co-doping effects using the wien2k.

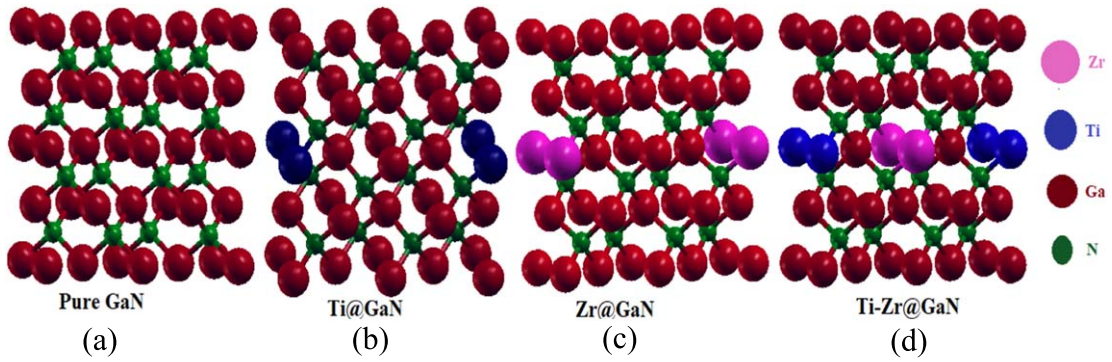

Figure 1. Supercell of (a) pure GaN, (b) Ti@GaN, (c) Zr@GaN and (d) Ti-Zr@GaN.

Search for materials for fabrication of electronic, photonic, and spintronic device is the main quest of researchers. Scientists are trying to propose new materials which could be potentially used for fulfilling the needs of the electronic and spintronic industry. Transition metals doping into semiconductors have been focused with great interest in developing material science due to the fact that they may enhance the reactivity properties and may bind strongly to nanomaterials [21]. Among the transition metals, Ti and Zr are considered as excellent dopants owing to their versatile and facile fabrication methods. They also yield rapid separation rates of charge carriers [22, 23]. Zirconium (Zr) is appraised for doping into semiconductors because of its unique properties including increased photoemission [24]. Literature review revealed that research on zirconium (Zr) doping into GaN is not conducted so much and yet more is to be investigated. Syyed Hassan Saberi *et al* [25] have studied (using PWSCF code) electronic structure and magnetic properties of transition metals doped GaN. They found a non-magnetic behavior of Zr doped GaN. Jia-Bin Li and Hong-Xia Li [26] theoretically investigated (using CASTEP code) transition metal doped GaN and found a non-magnetic character of Zr doped GaN. On the other hand, titanium (Ti) proved to bring surprising changes into electronic, optical, and magnetic properties of GaN [27, 28]. Titanium doping into GaN has earlier been reported in one of our research studies [29] where addition of Ti impurity brings magnetic character into GaN. Also, co-doping is expected to bring surprising changes into the optical, electronic and magnetic properties. It may further enhance stability of materials in comparison to mono-doping [30, 31]. Knowing the importance of Ti and Zr doping into GaN, in this research study, we performed co-doping of Ti and Zr into GaN (Ti-Zr@GaN). Hence, the current study is a computational study, in which we calculated the structural, electronic, magnetic, and optical properties of Zr doped and Ti-Zr co-doped GaN.

2. Computational method

Current research was performed using the Wien2k code [32, 33] based on the Perdew–Burke–Ernzerhof (PBE) generalized gradient (PBE-GGA) [34] approximations with the density functional theory (DFT). In the gallium nitride supercell ($1 \times 2 \times 2$), one Ga atom was substituted with one titanium (Ti)/zirconium (Zr) atom in order to realize supercell of Ti doped GaN (Ti@GaN) and Zr doped GaN (Zr@GaN). A concentration of 6.25% was obtained by doping Ti/Zr atoms into GaN while substitution was performed at second site Ga atom. Then Ti and Zr atoms were co-doped at second and fourth site in GaN supercell by substituting one Ga atom with Ti and another Ga atom with Zr atom (Ti-Zr@GaN). The supercells of pure GaN, Ti@GaN, Zr@GaN and Ti-Zr@GaN materials have been represented in figure 1. In the computational manipulation, the ($4p^1\ 3d^{10}$), ($2s^2\ 2p^3$), ($3d^2\ 4s^2$), and ($4d^2\ 5s^2$) states were supposed as the core states corresponding to Ga, N, Ti and Zr atoms. Ground state separation was chosen by taking -6 Ry value of energy separation. Angular momentum expansion value $l = 6$ was selected and potential is kept spherically symmetric within the muffin-tin sphere. The energy, charge, and force conversion values equal to 10^{-4} Ry, 10^{-2} C, and 1 mRy/a.u. were set for self-consistency criterion. 1200 k points were selected and relativistic effects were not included.

3. Results and discussions

3.1. Structural properties

Structural properties for the titanium doped, zirconium doped, and titanium-zirconium co-doped GaN were calculated using the optimizational procedure in the Wien2k code. Structural information was encoded in terms

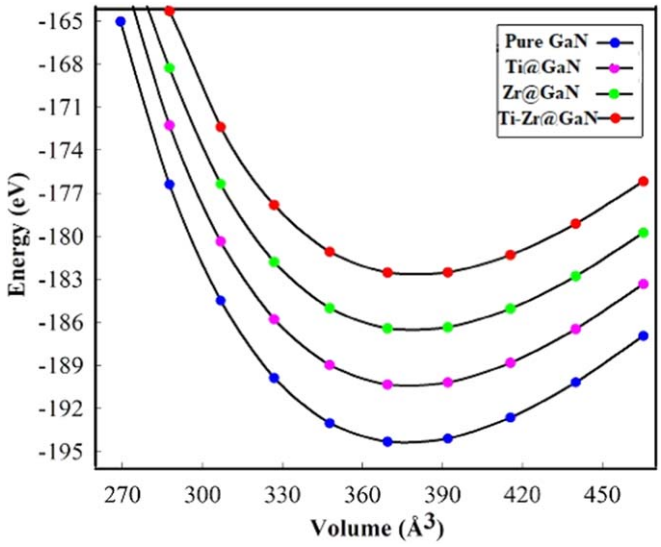

Figure 2. Volume optimization curves of pure GaN, Ti@GaN, Zr@GaN, and Ti-Zr@GaN.

Table 1. Lattice constants (a(Å)), bulk modulus (B_0), minimum equilibrium energy (E_0), and cohesive energy of pure GaN, Ti@GaN, Zr@GaN and Ti-Zr@GaN.

Materials	a(Å)	$B_\circ$(GPa)	E_{min}(eV)	$E_{cohesive}$(eV)
Pure GaN	4.53 [37, 39]	176.42 [40]	−194.33	−8.92 [45, 46]
Ti@GaN	4.96 [27, 29]	199.99 [27, 29]	−190.34	−11.95 [29]
Zr@GaN	4.94 [27, 29]	201.54 [27, 29]	−186.43	−6.89 [25, 46]
Ti-Zr@GaN	4.99 [27, 29]	205.98 [27, 29]	182.55	−7.52 [46]

of structural parameters including bulk modulus (B_0), minimum of total energy (E_0), and equilibrium volume (V_0). These parameters have been calculated using Murnaghan equation of states (EOS) [35, 36],

$$E(V) - E(V_0) = \frac{B_0 V}{B_0'}\left[\frac{(V_0/V)^{B_0'}}{B_0' - 1} + 1\right] - \frac{B_0 V_0}{B_0' - 1}.$$

These structure constants have been tabulated in table 1. Volume versus energy curves have been shown in figure 2. Optimized lattice constant of pure GaN estimated to be 4.53 Å which shows slight difference from values of lattice constants (4.49 Å, 4.54 Å) as calculated experimentally by T Lei *et al* [37] and M J Paisly *et al* [38], respectively. Calculated lattice constant of pure GaN have close resemblance with theoretical findings of Hongbo Qin *et al* [39] and M J Espitia R *et al* [40]. However, doping has caused significant change in lattice constant due to difference in ionic radii of dopants. In comparison to ionic radius of Ga ∼1.30 Å, larger ionic radius of dopants, Ti ∼1.40 Å and Zr ∼1.55 Å have caused slight expansion of lattice constant. Consequently, lattice constants of Ti@GaN, Zr@GaN and Ti-Zr@GaN have been obtained to be, 4.96 Å, 4.94 Å, and 4.99 Å, respectively (table 1). Moreover, bond length between Ga-N atoms was obtained to be 1.95 Å [25, 41]. However, upon substitution of Ti and Zr atoms with Ga atom, average bond distance between Ti-N and Zr-N estimated to be 2.01 Å [27, 29] and 2.32 Å [25, 26], respectively.

Bulk modulus is one of the critical parameter of any material and describes resistance of a material under compression. Values of bulk moduli have been listed in table 1. Value of bulk modulus for pure GaN (176 GPa) as calculated in our computational study have great resemblance with the theoretical findings of Hongbo Qin *et al* [39] and M. B. Kanoun *et al* [42]. On the other hand, values of bulk modulus for Ti, Zr and Ti-Zr co-substituted GaN have been found to increase in comparison to that of pure GaN. Titanium doped GaN has bulk modulus value of 199.99 GPa which however matches with $B_\circ$ values as calculated theoretically by M J Espitia Rico *et al* [27] and M. Junaid Iqbal Khan *et al* [29]. However, values of bulk moduli of Zr@GaN (201 GPa) and Ti-Zr co-doped GaN (205 GPa) may be compared with values reported in works where same group elements have been doped into GaN [27, 29] and these values may further be compared with pure GaN [39, 42]. Moreover, bulk moduli have been increased with dopants addition as, $B_\circ$(Pure GaN) < $B_\circ$(Ti@GaN) <

Table 2. Formation energies (E_f).

	Configuration	Ga-rich	N-rich
E_{fi} (eV)	Ti@GaN	5.65	−3.61
	Zr@GaN	−2.55	−4.43
	Ti-Zr@GaN	1.66	−4.16

B_o(Zr@GaN) < B_o(Ti-Zr@GaN) which means that Ti-Zr@GaN material much harder than other supposed materials.

Cohesive energy is a measure of strength of forces which bind atoms together and it describes stability of structure. According to Gaudoin *et al* [43], it is defined as energy which is equal to difference between total energy of compound and energy of individual atoms. It may be calculated using [44],

$$E_{cohesive} = (E_{total} - aE_{Ga} + bE_N + cE_{Ti/Zr/Ti-Zr})/(\mathrm{a} + \mathrm{b} + \mathrm{c})$$

Where, E_{total}, E_{Ga}, and E_N represent total energy of system, energy of isolated Ga and N atoms respectively. While, $E_{Ti/Zr/Ti-Zr}$ correspond to energies of Ti doped GaN, Zr doped GaN and Ti-Zr co-doped GaN, respectively. The constant numbers a, b, c, and d, represent the numbers of Ga, N, Ti/Zr/Ti-Zr atoms in the Ti@GaN, Zr@GaN, and Ti-Zr@GaN, respectively. Relative comparison among cohesive energies of all compounds has been tabulated in table 1. Cohesive energy values are however different from the cohesive energy of pure GaN as calculated theoretically by F. Benkabou *et al* [45], Maurizia Palummo *et al* [46] and Agostino Zoroddu *et al* [47].

3.2. Formation energies

We performed formation energy calculations of proposed materials with and without spin inclusion and found that spin polarized calculations are more favorable than non-spin polarized calculations. Formation energies of Ti/Zr materials have been calculated using,

$$E_{f1} = E_{Ti/Zr@GaN} - E_{GaN} + \mu_{Ga} + \mu_N - \mu_{Ti/Zr}$$

Where $E_{Ti/Zr}$ and E_{GaN} are the energies corresponding to total energies of Ti@GaN, Zr@GaN, and pure GaN, respectively. μ_{Ga}, μ_N, and $\mu_{Ti/Zr}$ are the chemical potentials of Ga, N, Ti, and Zr atoms in their stable bulk structure. To check stable configuration, we have calculated the formation energies of single Ti/Zr atoms doped GaN. The μ_{Ga} depends on the experimental growth condition, Ga-rich and N-rich. To estimate the chemical potential, we have used the $\mu_{GaN} = \mu_{Ga} + \mu_N$, relation where μ_{Ga} and μ_N represent the chemical potentials of Ga and N, respectively. μ_{GaN} can be considered as the total energy of pure GaN per formula unit (E_{GaN}). μ_{Ga} for the Ga-rich environment is equal to E_{Ga}, where E_{Ga} is the total energy of Ga per atom in the structure. Thus, we can compute μ_N for the Ga-rich environment from $\mu_{GaN} - \mu_{Ga}$. For the N-rich condition, μ_N is equal to E_N, where E_N is the total energy of N per atom in the cubic crystal structure. Therefore, μ_{Ga} can be calculated for the N-rich environment as $\mu_{GaN} - \mu_N$. Formation energies of Ti@GaN and Zr@GaN materials have been tabulated in the table 2. From table 2, it may be observed that the formation energies under the N-rich condition for Ti/Zr@GaN are negative and lower than those under the Ga-rich condition which means that Ti/Zr atoms can be easily incorporated into GaN under the N-rich condition due to lower formation energy [48].

Similarly, we have calculated the stability of the Ti-Zr co-doped GaN using,

$$E_{f2} = E_{Ti-Zr@GaN} - E_{GaN} + \mu_{Ga} - \mu_{Ti} - \mu_{Zr}$$

Where $E_{Ti-ZrGaN}$, and E_{GaN} are the total energies of Ti-Zr@GaN, and pure GaN, respectively. μ_{Ga}, μ_{N}, μ_{Ti} and μ_{Zr} are the chemical potentials of Ga, N, Ti, and Zr, atoms, respectively. The formation energies are estimated to be 1.66 eV and −4.16 eV under the Ga-rich and N-rich conditions, respectively. The negative formation energy indicated the easy fabrication of Ti-Zr@GaN in the experiment under the N-rich environment.

3.3. Electronic and magnetic properties

We performed spin polarized calculations and calculated partial density of states (PDOS) along with total density of states (TDOS). Vertical dotted line represents the Fermi level. We studied DOS behavior during −5 eV to 5 eV. The density of states of pure GaN has been shown in figure 3(a) where symmetric DOS distribution was observed for both spin up and spin down channels. Symmetric DOS indicate non-magnetic character of GaN, having zero magnetic moment. DOS analysis revealed that only Ga *d*-states and N *p*-states are influential so we have only plotted these orbitals in DOS plots of pure GaN. It is consistent with the research findings of Jiabin Li and Hongxia Liu [49], M Umair Farooq *et al* [50] and E Maskar *et al* [51].

On the other side, for the Ti@GaN, Zr@GaN and Ti-Zr@GaN materials, we have plotted only highly contributing orbitals of Ga, N, Zr, and Ti atoms in order to provide more clarity in discussion of DOS. Partial

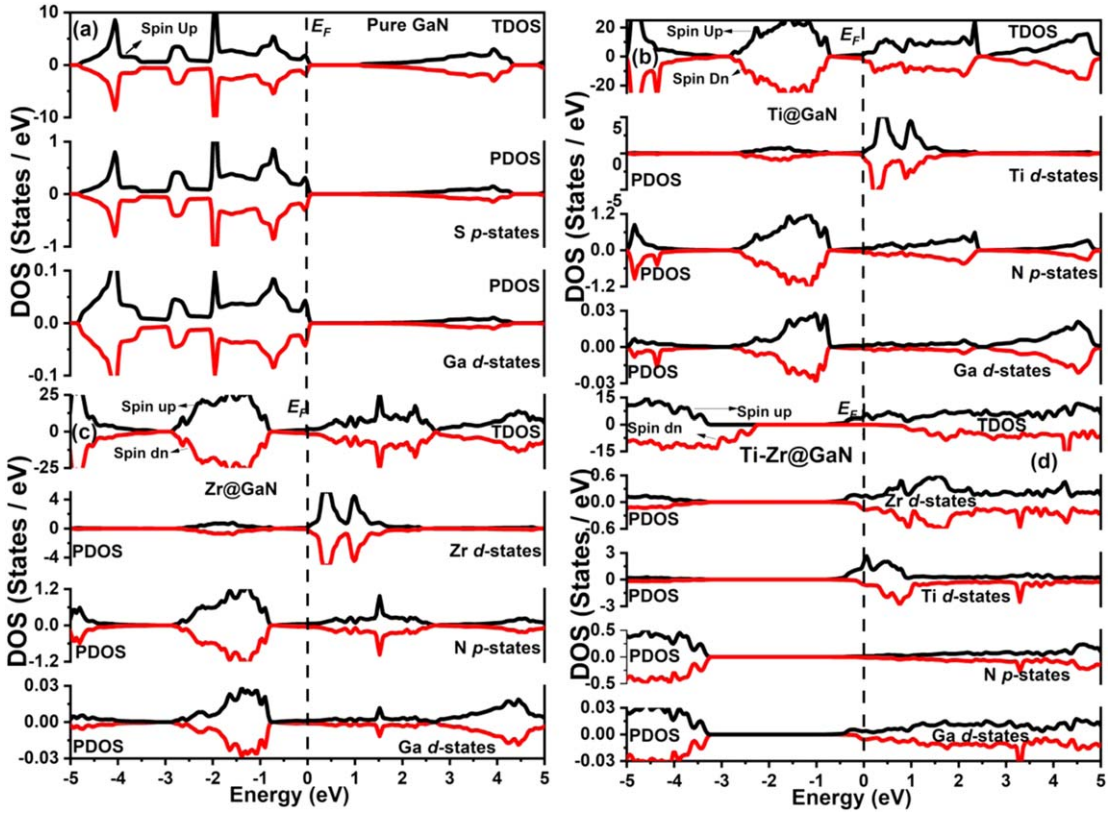

Figure 3. Density of states (DOS) of (a) pure GaN, (b) Ti@GaN, (c) Zr@GaN, and (d) Ti-Zr@GaN. Vertical dotted line represents Fermi level.

and total density of states of Ti doped GaN have been shown in figure 3(b) where both spin channels of Ti 3*d*, Ga 3*d*, and N 2*p*-states found to be asymmetric. Asymmetry of states represents magnetism in the Ti@GaN. However, significant contribution of Ti 3*d*-states has been noticed and is responsible for tuning electronic behavior of Ti@GaN material. Similar spin polarized DOS trends have been reported in the study of Victor Mendoza-Estrada *et al* [52], Miguel J Espitia R. *et al* [53] and Zhihua Xiong *et al* [54]. Density of states shows symmetric distribution for Zr doped GaN during −5 eV to 5 eV, energy range (figure 3(c)). In the valence band, Ga 3*d*-states, N 2*p*-states and Zr 4*d*-states are localized in −2.9 eV to −0.7 eV. In the conduction band, Ga *d*-states, N *p*-states, and Zr *d*-states are located in 0–2.4 eV but prominent behavior of Zr 4*d*-states is remarked. Zr 4*d*-states vanished almost during −5 eV to −2.9 eV, −0.7 eV to −0.2 eV, and 2.4 eV to 5 eV, energy ranges. However, non-magnetic character of Zr@GaN is obtained in this research study which matches with already published research works of S H Saberi *et al* [25] and Jia-Bin Li and Hong-Xia Liu [26]. In addition, Ti and Zr co-doped GaN have shown asymmetric DOS behavior in conduction and valence band which points magnetism in this material. In the valence band, Ga *d*-states and N *p*-states are observed in the low energy region (−5 eV to −3.2 eV). The 3*d*-states of Ti and Zr 4*d*-states were not noticed in −3.2 eV to −0.6 eV but these states are localized around Fermi level which consequently enhanced electronic properties of Ti-Zr@GaN. DOS behavior of Ti-Zr@GaN resembled already reported other transition metal co-doped GaN materials [28, 29]. Moreover, hybridization of *d*-states of dopants and *p*-states of N atoms is observed.

In our study, symmetric distribution of spin up and spin down states was observed in DOS plot of pure GaN (indicating zero magnetic moment) and it match with the reported works [49, 51]. Zirconium doped GaN materials obtained to be symmetric which suggested its nonmagnetic character. Absence of magnetism into Zr@GaN material as obtained in our research matches well with the study of Seyyed Hassan Saberi *et al* [25] but it did not match with the result of Jia-Bin Li and Hong-Xia Liu [26]. However, magnetism was observed upon doping Ti into GaN and Ti-Zr co-doped GaN. Total magnetic moment of Ti doped GaN as obtained in our research is 0.99 μ_B and it may be well compared with research study of Miguel J Espitia R *et al* [53]. It was revealed that major contribution of magnetic moment emerged from Ti atom (0.644 μ_B) while Ga and N atoms have moment values of 0.128 μ_B and 0.001 μ_B, respectively. However, total magnetic moment of Ti-Zr@GaN material is 1.503 μ_B with magnetic moment values of titanium and Zr atoms, 0.856 μ_B, 0.218 μ_B, respectively. So, both the titanium and zirconium atoms played a major role in producing magnetic character into Ti-Zr@GaN. Values of total magnetic moments of the selected materials have been enlisted in table 3.

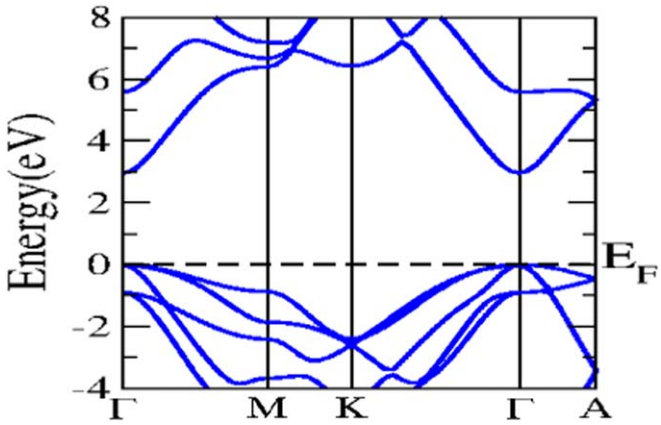

Figure 4. Band gap of pure GaN obtained using Tb-mbj.

Table 3. Calculated magnetic moments of pure GaN, Ti@GaN, Zr@GaN and Ti-Zr@GaN.

Materials	$\mu^{\text{interstitial}}(\mu_B)$	$\mu^{Ga}(\mu_B)$	$\mu^{N}(\mu_B)$	$\mu^{Ti}(\mu_B)$	$\mu^{Zr}(\mu_B)$	$\mu^{Total}(\mu_B)$
Pure GaN	0	0	0	—	—	0 [49, 51]
Ti@GaN	0.217	0.128	0.001	0.644		0.99 [53]
Zr@GaN	0	0	0	—	0	0 [25]
Ti-Zr@GaN	0.426	0.002	0.001	0.856	0.218	1.503

3.4. Band structure

Band gap of semiconductors helps in estimating technological uses of these materials in the field of optoelectronics, photonics, and power electronics. Band gap of binary semiconductors including GaN enables their uses for fabrication of most of commercial optoelectronics and photonic devices. To overcome the band gap problem, we have employed the Trans-Blaha-modified Becke-Johnson (TB-mBJ) method, as it is considered to estimate the band gap near to the experimental value as reported by Fabien Tran and Peter Blaha [55]. To begin, we looked at the band structure of pure GaN using the TB-mBJ potential, as displayed in figure 4. Our calculations demonstrate that pure GaN possesses a semiconducting nature with a band gap of 2.96 eV, which is in close agreement with the experimental value as reported in study of T Lei *et al* [37] and Stephan Lany and Alex Zunger [56]. Our calculated value of band gap may further be compared with experimentally calculated value by Benjamin W Jacobs *et al* [57]. The valence band maximum (VBM) and conduction band minimum (VBM) lies at the same symmetry point Γ as shown in figure 4 indicating that GaN has a direct band gap. Our Tb-mbj calculated band gap value has great resemblance with theoretical findings of Rafael B Araujo *et al* [58].

Consequent upon addition of Ti, Zr, and Ti-Zr impurities into the GaN, shrinkage of bands have been observed. Doping of impurities (Ti/Zr/Ti-Zr) into GaN has caused generation of states in the conduction band and these states overlap with each other, indicating conducting nature of selected materials. However, role of dopants *d*-states as observed in DOS plots, have significantly tuned electronic response of these materials. Scope of these materials has been extended to the fields of device fabrication and design of photonic and power electronic devices.

3.5. Optical properties

After understanding the electronic behavior of pure GaN, Ti@GaN, Zr@GaN and Ti-Zr@GaN, we further moved to calculate their optical response as it has direct dependence upon variation in electronic behavior. We calculated optical constants including optical absorption (α), conductivity (σ), refractive index (n), real dielectric (ε_r), extinction coefficient (k) and reflectivity (R) of these materials. Optical properties changes because of interband transitions and most of the information about transitions has been related to dielectric function $\varepsilon(\omega) = \varepsilon_r(\omega) + i\varepsilon_i(\omega)$ [59, 60]. Since, all of optical properties have been calculated in term of $\varepsilon(\omega)$ so that is why we may see a clear evidence of optical transitions in each plot in term of various peaks.

Optical absorption is the fundamental parameter which precisely incorporates photoresponse of any material upon its interaction with the electromagnetic radiations. Theoretically, it is calculated in term of real ($\varepsilon_r(\omega)$) and imaginary ($\varepsilon_i(\omega)$) parts of dielectric constant ($\varepsilon(\omega)$) [29],

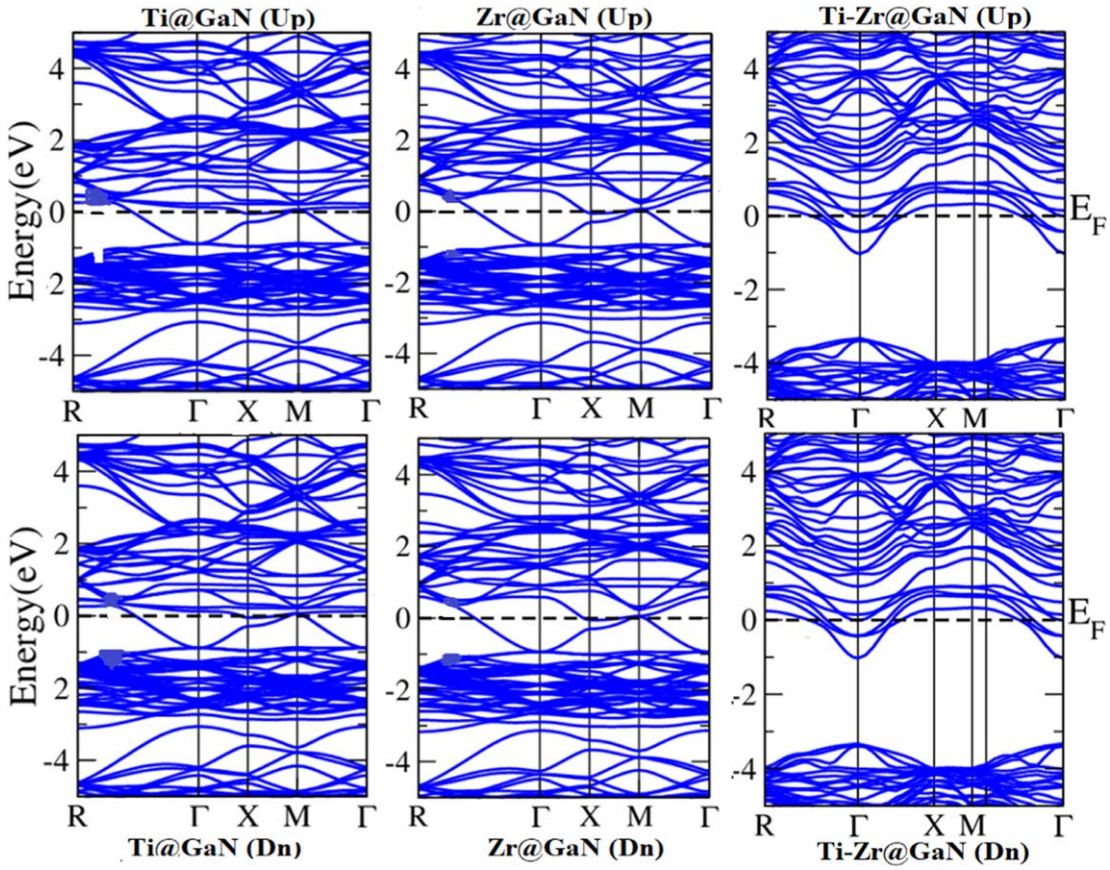

Figure 5. Band gap of Ti@GaN, Zr@GaN and Ti-Zr@GaN. Top panel represent spin up states and down panel represent spin dn states..

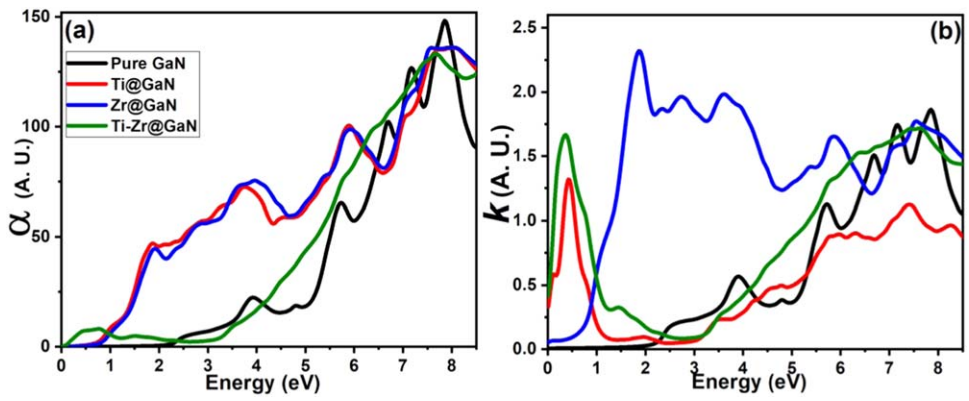

Figure 6. Optical (a) absorption, (b) extinction coefficient of pure GaN, Ti@GaN, Zr@GaN and Ti-Zr@GaN

$$\alpha(\omega) = \sqrt{2}\,[\sqrt{\varepsilon_r^2(\omega) + \varepsilon_i^2(\omega)} - \varepsilon_r(\omega)]^{1/2}$$

Frequency dependent absorption spectra of zirconium doped GaN and Ti-Zr co-doped GaN have been shown in figure 6(a). Impurities addition causes prominent changes in the absorption traits upon comparison to pure GaN. Absorption of pure GaN increased with increase in photon energy and has maximum absorption at 7.87 eV (~ 157.54 nm). However, absorption did was not observed below 2.25 eV which means lower energy photons are not well absorbed inside GaN. Absorption trends for pure GaN matches with study of J. O. Akinlami and I. O Olateju [61]. Absorption spectra of pure GaN also matched with work reported by J F Muth *et al* [62]. Absorption of titanium doped GaN increases with increase in photon energy and demonstrates maximum absorption at 8.06 eV (~ 153.86 nm). After attaining maximum absorption, absorption starts decreasing but becomes constant for higher energy values. Photons having energy energies in range (0–0.67 eV) do not cause

any absorption in Ti@GaN. Our findings are supported with the results of Zhen Cui *et al* [28] and M Junaid Iqbal Khan *et al* [29]. Zero photoresponse of Zr doped GaN was observed between 0–0.77 eV but this material absorbs photons having energies higher than 0.77 eV until maximum absorption is observed at 8.0 eV. This absorption shoulder is shifted to higher energy in comparison to maximum absorption (7.87 eV) of pure GaN and thus exhibits blueshift [28, 29]. Similar absorption trend and blueshift has been noticed while doping zirconium into other semiconductor [63, 64]. Blueshift may be attributed to strong bonding and may be related to defects in lattice which causes change in bonding among various atoms. It may emerge due to nanostructure formation and increase in particle size [65]. On the other hand, Ti-Zr co-doped GaN absorbs photon even at lower frequencies and an extended absorption edge is observed in 0–1.19 eV. Almost a constant absorption trend is noticed during the 1.19–2.98 eV energy range which after 2.98 eV, rises suddenly until maximum absorption is noted at 7.7 eV. Absorption edge is shifted to lower energies in comparison to pure GaN and thus, redshift is observed. Absorption maxima for Zr@GaN and Ti-Zr@GaN were obtained at energies, 1.9, 2.83, 3.95, 5.85, 8.0 eV, and 0.6, 1.52, 7.7 eV, respectively. Absorption maxima of these selected materials indicate good absorption at these energy values. Titanium substitution into GaN shifted the absorption edge to higher energies as found in our already published research [29] but Ti and Zr co-doping into GaN shifts the absorption edge to lower energies, causing redshift. However, both materials have excellent photoresponse in the UV region. Emerging absorption trend of Ti-Zr@GaN material in the low energy region may be associated with quantum confinement effects [29]. Extended peaks occurring in the Ti-Zr@GaN material may be the effect of co-doping and interband transitions. Improvement in the absorption spectra of these materials may emerge due to states which are generated into the GaN after adding zirconium and Ti-Zr co-doping. Absorption trends of Zr@GaN and Ti-Zr@GaN have great resemblance with absorption spectra of other transition metals doped semiconductors [66, 67]. Moreover, photoresponse of these materials may be controlled and tuned to our desired frequency range by adjusting the proportion of dopants.

Plot depicting extinction trends of Ti@GaN, Zr@GaN and Ti-Zr@GaN have distinct trends in comparison to pure GaN figure 6(b). Extinction coefficient may be calculated using [29].

$$k = \frac{\alpha\lambda}{4\pi}$$

Extinction maxima for pure GaN, Ti@GaN, Zr@GaN and Ti-Zr@GaN (1.87, 1.33, 2.33, 1.73) have been observed at 7.85 eV [61], 0.42 eV [28], 1.85 eV and 7.6 eV, respectively. These extinction edges emerged due to effect of impurities and shows maximum light absorption. A notable thing in extinction plot is that extinction maxima for Ti@GaN and Zr@GaN found in low energy region whereas k maximum value for pure GaN was observed in the UV region [28, 29]. Extinction edges were the result of efficient light absorption. However, extinction values as calculated in our research study lies in 0–0.41. Extinction trends obtained in current study matches with [28]. Moreover, relative absorption and scattering may be conceived from the extinction plots which may further guide us to find material applicability in the photonic, solar and allied devices.

Optical conductivity response of these materials along with change in energy of photons has been illustrated in figure 7(a). Optical conductivity may be calculated using [29],

$$\sigma(\omega) = -\mathrm{i}\frac{\omega}{4\pi}(\varepsilon(\omega) - 1).$$

Optical conductivity of pure GaN has maximum absorption at 7.09 eV but shows zero absorption in 0–2.2 eV. Conductivity trends of pure GaN matches well with the work reported by Zhen Cui *et al* [28] and Yujie Du *et al* [68]. While, we did not observe any conductivity traces of Ti doped GaN material in 0–0.56 eV but it is maximum at 7.45 eV. After 7.45 eV, conductivity suddenly decreased owing to least absorption. Conductivity trends of Ti@GaN material matches with the work of M Junaid Iqbal Khan *et al* [29] and may further be compared with pure GaN [28, 68]. In comparison to pure GaN [28, 68], notable variations in conductivity spectra of zirconium doped GaN and Ti-Zr@GaN have been observed. Conductivity maxima for Zr@GaN and Ti-Zr@GaN exist at 7.44 eV and 7.35 eV, respectively. Conductivity of Zr@GaN is zero in 0–0.65 eV energy range. Both materials showed enhanced conductivity in the UV region. Conductive response of these materials in the low energy range is the result of interband transitions. However, conductivity response is decreased in some regions and it may appear due to improper light absorption. Ti-Zr co-doped GaN exhibited best conductivity in the UV region and such behavior may have a good comparison to other transition metals co-doped semiconductor systems [69, 70]. Moreover, DOS variations caused prominent variations in conductivity plots and shifting of conductivity edges may be caused by *p-d* hybridization (figure 3).

Refractive indices ($n(\omega)$) of pure GaN, titanium doped, zirconium doped and Ti-Zr co-doped GaN have been shown in figure 7(b). Refractive indices may be calculated using [29],

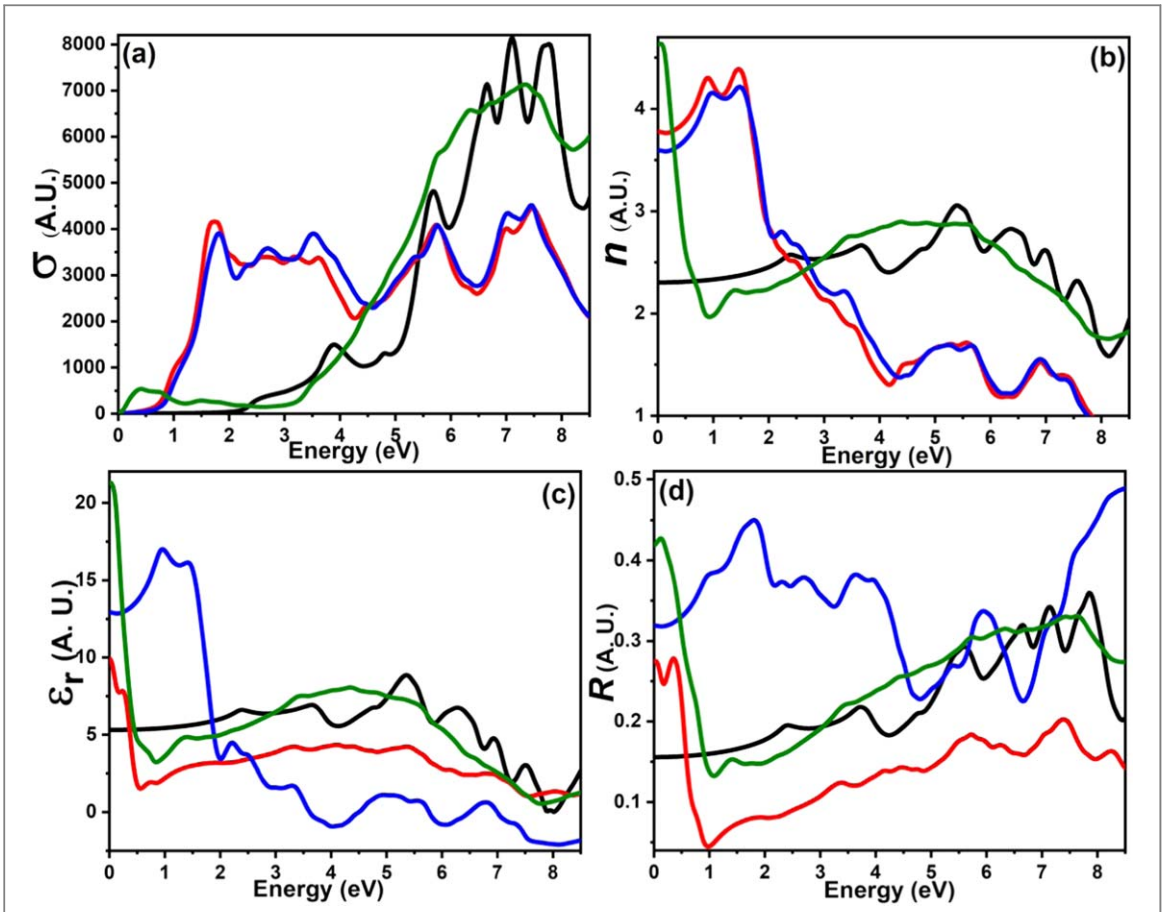

Figure 7. Optical constants including (a) conductivity, (b) refractive index, (c) real dielectric, and (d) reflectivity of pure GaN, Ti@GaN, Zr@GaN and Ti-Zr@GaN

$$n(\omega) = \left[\frac{\varepsilon_1(\omega)}{2} + \frac{\sqrt{\varepsilon_1^2(\omega) + \varepsilon_2^2(\omega)}}{2}\right]^{\frac{1}{2}}$$

Distinct n trends for both the materials have been noticed in 0–8.5 eV. At first instance, it has been observed that refractive indices trends showed oscillatory trends. These oscillatory trends may emerge as the result of excitonic transition and because of light absorption at different energies. But static values of refractive indices of pure GaN, Ti@GaN, Zr@GaN and Ti-Zr@GaN were observed to be 2.3 [28, 68], 3.78 [29], 3.6 and 4.6, respectively. These static n values are larger than the value of n for pure GaN [29]. It is worthy to mention here that the $n(0)$ value for Ti-Zr@GaN is larger than its static counterpart for Ti@GaN [28, 29] and it may be due to the effect of co-doping. Maximum refractive index value (4.21) for Zr@GaN has been obtained 1.51 eV. Calculated value of refractive index in current research (2.79) at 1.99 eV (623.04 nm) has good agreement with n value obtained in the research study of Soner Özen [24]. Differences between two research studies lie within the provision of theoretical (DFT) and experimental procedures. Decreasing trend in n values at different energies represent denser medium and it may be further related to density of states (DOS) as observed in figure 3.

The real dielectric constant ($\varepsilon_r(\omega)$) shows response of material in term of polarization upon interaction with electromagnetic light. Kramers-Kroning transform of imaginary part of dielectric constant ($\varepsilon(\omega)$) yields real dielectric constant [29],

$$\varepsilon_r(\omega) = 1 + \frac{2}{\pi}\rho_0 \int_{\infty}^{0} \frac{\omega/\varepsilon_i(\omega)}{\omega/^2 - \omega^2} d\omega/.$$

Energy dependent dielectric spectra have been shown in figure 7(c) and an elaborative comparison of real dielectric plots of pure GaN, Ti@GaN, Zr@GaN, and Ti-Zr@GaN materials has been presented. Real static dielectric constant of selected materials have shown an increase in comparison to pure GaN [28, 29]. Static values of real dielectric constant of pure GaN, Ti@GaN, Zr@GaN and Ti-Zr@GaN were observed to be, 5.37 [28, 61], 9.9 [28, 29], 12.86 and 21.35, respectively. These values are greater than $\varepsilon_r(0)$ for pure GaN. Higher dielectric values were observed for Ti@GaN, Zr@GaN and Ti-Zr@GaN and may appear due to high charge

carriers. The real dielectric constant of Ti-Zr co-doped GaN may be compared with one of our already reported research [29]. However, at higher energies (frequencies) a nominal decrease in dielectric constant was observed which may be due to presence of dipoles which are not aligned with the external field at the higher energies. Similar dielectric trends are noticed in the studies of transition metals doped semiconductors [71, 72].

Reflection of electromagnetic radiations from material surface indicates least absorption inside the material. Knowing usefulness of reflectivity in characterizing materials for various optical purposes, we theoretically calculated it using [28],

$$R(\omega) = \left[\frac{\sqrt{\varepsilon_1(\omega) + i\varepsilon_2(\omega)} - 1}{\sqrt{\varepsilon_1(\omega) + i\varepsilon_2(\omega)} + 1}\right]^2$$

Reflectivity behavior of pure GaN, Zr@GaN, and Ti-Zr@GaN has been understood in 0–8.5 eV (figure 7(d)). Static reflectivity, measured at zero frequency (R(0)) corresponding to pure GaN, Ti@GaN, Zr@GaN, and Ti-Zr@GaN have 0.15, 0.27, 0.31, and 0.41 values, respectively. Reflectivity varies with photons of different energies however, reflectivity maxima (0.36, 0.28, 0.48, 0.43) have been observed at energies, 7.86 eV (∼ pure GaN), 0.35 eV (∼Ti@GaN), 8.45 eV (∼Zr@GaN) and 0.12 eV (∼Ti-Zr@GaN), respectively. Reflectivity behavior (trend) of zirconium doped GaN have a close resemblance with the work reported by Soner Özen [24] in their experimental study. A sudden decrease in reflectivity of Ti-Zr@GaN has been witnessed in 0.43–1.0 eV which on other hand, indicates good absorption of electromagnetic light in this region as observed in figure 6(a). Moreover, the reflectivity trend of Ti-Zr co-doped GaN shows a clear difference from the reflectivity plot of Ti doped GaN [29] and it may possibly be due to the effect of co-doping.

4. Conclusion

In current research, we calculated structural, electronic, magnetic, and optical properties of Zr@GaN and Ti-Zr co-doped GaN. Perdew–Burke–Ernzerhof (PBE) generalized gradient approximation (GGA) has been employed within Wien2k code. Lattice parameters were slightly enlarged due to substitution of impurities into GaN. Electronic properties were greatly enhanced by the Ti 3*d*, Zr 4*d* and Ga 3*d*, and N 2*p*-states. *p-d* hybridization was observed which enhanced mobility of electrons in conduction process. Zr substitution into GaN does not bring magnetism into GaN while Ti@GaN and Ti-Zr co-doping into GaN, turns it magnetic with magnetic moments values of 0.99 μ_B and 1.503 μ_B, respectively. Substitution of Ti/Zr into GaN may be more favorable at N-rich conditions due to lower formation energy. Blueshift in absorption spectrum of Ti@GaN and Zr@GaN was noticed while a redshift was observed with Ti-Zr co-doping. Absorption spectra for both the materials were significantly enhanced in the UV region, leading towards their potential uses in the UV optoelectronics and in solid state nano-emitters.

Data availability statement

The data that support the findings of this study are available upon reasonable request from the authors.

ORCID iDs

M Junaid Iqbal Khan https://orcid.org/0000-0002-8051-7098
Juan Liu https://orcid.org/0000-0002-9709-7894
Imran Taj https://orcid.org/0000-0002-2322-5566
Hamid Ullah https://orcid.org/0000-0001-7304-8863
Masood Yousaf https://orcid.org/0000-0001-9862-1072

References

[1] Morkoc H, Strite S, Gao G B, Lin M E, Sverdlov B and Burns M 1994 Large-band-gap SiC, III-V nitride, and II-VI ZnSe-based semiconductor device technologies *J. Appl. Phys.* **76** 1363–98
[2] Strite S, Lin M E and Morkoc H 1993 Progress and prospects for GaN and the III–V nitride semiconductors *Thin Solid Films* **231** 197–210
[3] Oğuzman I H, Bellotti E and Brennan Kevin F 1997 Theory of hole initiated impact ionization in bulk zincblende and wurtzite GaN *J. Appl. Phys.* **81** 7827–34
[4] Mietze C, Landmann M, Rauls E, Machhadani H, Sakr S, Tchernycheva M, Julien F H, Schmidt W G, Lischka K and As D J 2011 Band offsets in cubic GaN/AlN superlattices *Phys. Rev. B* **83** 195301
[5] Berdalovic I, Poljak M and Suligoj T 2021 A comprehensive model and numerical analysis of electron mobility in GaN-based high electron mobility transistors *J. Appl. Phys.* **129** 064303

[6] Xu Gaofeng, David Cao Jiayu, Labinac Velimir and Zutic Igor 2021 Intensity equations for birefringent spin lasers *Phys. Rev. B* **103** 045306
[7] Krames M R, Shchekin O B, Mueller-Mach R, Mueller G O, Zhou L, Harbers G and George Craford M 2007 Status and future of high-power light-emitting diodes for solid-state lighting *JDT.* **3** 160–75
[8] Qi L, Zhang X, Chong W C, Li P and Lau K M 2021 848 Ppi high-brightness active-matrix micro-LED micro-display using GaN-on-Si epi-wafers towards mass production *Opt.* **29** 10580–91
[9] Song W, Chen J, Li Z and Fang X 2021 Self-powered MXene/GaN van der Waals heterojunction ultraviolet photodiodes with superhigh efficiency and stable current outputs *Adv. Mater.* **33** 2101059
[10] Furqan C M, Khan M U, Awais M, Jiang F, Bae J, Hassan A and Kwok H S 2021 Humidity sensor based on Gallium Nitride for real time monitoring applications *Sci.* **11** 1–14
[11] Kim K, Wu F, Wise K D and Yoon E 2021 GaN-on-silicon MicroLEDs for neural interfaces *Semicond.* **106** 123–72
[12] Parbrook P J, Corbett B, Han J, Seong T-Y and Amano H 2021 Micro-light emitting diode: from chips to applications *Laser Photonics Rev.* **15** 2000133
[13] Yuan S, Sheng Y, Liu C, Yu L, Dong L, Xing F, Zhang J, Di Y and Gan Z 2021 Fluorescence enhancement of perovskite nanocrystals by flexible photonic crystals and its application in optical strain gauge *Appl. Phys. Lett.* **119** 033302
[14] Yuan T, Fu C, Gong Y, Tong Y, Zhang J and Wang Y 2021 First-principles insights into Cu-decorated GaN monolayers for sensing CO and HCHO in Dry-Type transformers *ACS omega.* **6** 19127–33
[15] Lyons J L, Glaser E R, Ellen Zvanut M, Paudel S, Lwinska M, Sochacki T and Bockowski M 2021 Carbon complexes in highly C-doped GaN *Phys. Rev. B* **104** 075201
[16] Li H-L, Xie R-J, Hirosaki N, Dierre B, Sakiguchi T and Yajima Y 2008 Preparation and cathodoluminescence of Mg-Doped and Zn-Doped GaN powders *J. Am. Ceram. Soc.* **91** 1711–4
[17] Khan M J I, Kanwal Z, Yousaf M, Ullah H, Ahmad J, Latif A, Shin Y-H and Khalid A U R 2021 Effect of Zn doping on electronic structure and optical properties zincblende GaN (A DFT + U insight) *Commun. Theor. Phys.* **73** 035701
[18] Wang J, Zhang X, Liu L and Wang Z 2021 Dissolved gas analysis in transformer oil using Ni-Doped GaN monolayer: a DFT study *Superlattices Microstruct.* **159** 107055
[19] Kumar Jain S *et al* 2021 2D/3D Hybrid of MoS_2/GaN for a high-performance broadband photodetector *ACS Appl. Electron. Mater.* **3** 2407–14
[20] Dubey A, Mishra R, Hsieh Y-H, Cheng C-W, Wu B-H, Chen L-J, Gwo S and Yen T-J 2020 Aluminum plasmonics enriched ultraviolet GaN photodetector with ultrahigh responsivity, detectivity, and broad bandwidth *Adv. Sci.* **7** 2002274
[21] Weiss C *et al* 2020 Toward nanotechnology-enabled approaches against the COVID-19 pandemic *ACS Nano.* **14** 6383–406
[22] Sun Z, Fang G, Li J, Mo J, He X, Wang X and Yu Z 2020 Preparation of (Ti, Zr) co-doped hematite photoanode for enhanced photoelectrochemical water splitting *Chem. Phys. Lett.* **754** 137736
[23] Wu Q, Meng D, Zhang Y, Zhao Q, Bu Q, Wang D, Zou X, Lin Y, Li S and Xie T 2019 Acid-treated Ti4 + doped hematite photoanode for efficient solar water oxidation–Insight into surface states and charge separation *J. Alloys Compd.* **782** 943–51
[24] Soner Ö 2019 Zr-doped GaN thin films grown onto glass and PET substrates by thermionic vacuum arc *Mater. Res. Express* **6** 046401
[25] Hassan Saberi S, Mahdy Baizaee S and Kahnouji H 2014 Electronic structure and magnetic properties of transition-metal (Y, Zr, Nb, Mo, Tc, Ru, Rh, Pd, Ag and Cd) doped in GaN nanotubes *Superlattices Microstruct.* **74** 52–60
[26] Li J-B and Liu H-X 2018 Theoretical research of diluted magnetic semiconductors: GaN monolayer doped with transition metal atoms *Superlattice Microstruct.* **120** 382–8
[27] Espitia Rico M J, Sanchez P L C and Salcedo Parra O 2019 Structural and magnetic in c-AlN and c-GaN compound doped with Ti *J. Phys.:Conf. Ser.* **1386** 012028
[28] Cui Z, Ke X, Li E and Liu T 2016 Electronic and optical properties of titanium-doped GaN nanowires *Mater. Des.* **96** 409–15
[29] Khan M J I, Kanwal Z, Latif A, Ahmad J, Akhtar P, Yousaf M and Ullah H 2021 Investigations on electronic structure, magnetic and optical properties of C and Ti co-doped zincblende GaN for optoelectronic applications *Optik* **231** 166425
[30] Pan H, Gu B, Eres G and Zhang Z 2010 *Ab initio* study on noncompensated CrO codoping of GaN for enhanced solar energy conversion *J. Chem. Phys.* **132** 104501
[31] Korotkov R Y, Gregie J M and Wessels B W 2001 Electrical properties of p-type GaN: Mg codoped with oxygen *Appl. Phys. Lett.* **78** 222–4
[32] Blaha P, Schwarz K, Sorantin P and Trickey S B 1990 Full-potential, linearized augmented plane wave programs for crystalline systems *Comput. Phys. Commun.* **59** 399–415
[33] Kohn W and Sham L J 1965 Self-consistent equations including exchange and correlation effects *Phys. Rev.* **140** A1133
[34] Perdew J P, Burke K and Ernzerhof M 1996 Generalized gradient approximation made simple *Phys. Rev. Lett.* **77** 3865
[35] Francis B 1947 Finite elastic strain of cubic crystals *Phy. Rev.* **71** 809
[36] Murnaghan F D 1944 The compressibility of media under extreme pressures *PNAS* **30** 244
[37] Lei T, Fanciulli M, Molnar R J, Moustakes T D, Graham R J and Scanlon J 1991 Epitaxial growth of zinc blende and wurtzitic gallium nitride thin films on (001) silicon *Appl. Phys. Lett.* **59** 944–6
[38] Paisley M J, Sitar Z, Posthill J B and Davis R F 1989 Growth of cubic phase gallium nitride by modified molecular-beam epitaxy *J. Vac. Sci. Technol.* **7** 701–5
[39] Qin H, Luan X, Feng C, Yang D and Zhang G 2017 Mechanical, thermodynamic and electronic properties of wurtzite and zinc-blende GaN crystals *Mater.* **10** 1419
[40] Espitia M J, Ortega-López C and Martínez J A 2016 DFT applied to the study of carbon-doped zinc-blende (cubic) GaN *J. Phys. Conf. Ser.* **743** 012005
[41] Li H *et al* 2010 Electronic structures and magnetic properties of GaN sheets and nanoribbons *J. Phys. Chem. C* **114** 11390–4
[42] Kanoun M B, Goumri-Said S, Merad A E, Cibert J and Aourag H 2004 Zinc-blende AlN and GaN under pressure: structural, electronic, elastic and piezoelectric properties *Semicond. Sci. Tehnol.* **19** 1220
[43] Gaudoin R, Foulkes W M and Rajagopal G 2002 *Ab initio* calculations of the cohesive energy and the bulk modulus of aluminium *J. Phys.:Condens. Mater.* **14** 8787
[44] Zhang T, Yin H, Zhang C, Zhang R, Jiang X, Zheng Q and Qu X 2019 First-principles study on the mechanical properties and electronic structure of V doped WCoB and W2CoB2 ternary borides *Mater.* **12** 967
[45] Benkabou F, Becker P, Certier M and Aourag H 1998 Structural and dynamical properties of zincblende GaN *Phys. Status Solidi B Basic Res.* **209** 223–33
[46] Palummo M, Bertoni C M, Reining L and Finocchi F 1993 The electronic structure of gallium nitride *Phys. Rev. B: Condens. Matter* **185** 404–9

[47] Zoroddu A, Bernardini F, Ruggerone P and Fiorentini V 2001 First-principles prediction of structure, energetics, formation enthalpy, elastic constants, polarization, and piezoelectric constants of AlN, GaN, and InN: Comparison of local and gradient-corrected density-functional theory *Phys. Rev. B* **64** 045208
[48] Junaid Iqbal Khan M, Kanwal Z, Yousaf M, Nabi A, Ahmad J, Latif A and Ullah H 2020 Investigating structural, electronic and optical properties of CdS: Cr (A GGA and GGA + U study) *Solid State Sci.* **108** 106437
[49] Li J and Liu H 2018 Magnetism investigation of GaN monolayer doped with group VIII B transition metals *J. Mater. Sci.* **53** 15986–94
[50] Umair Farooq M, Atiq S, Zahir M, Salman Kiani M, Ramay S M, Zou B and Zhang J 2020 Spin-polarized exciton formation in Co-doped GaN nanowires *Mater. Chem. Phys.* **245** 122756
[51] Maskar E, Fakhim Lamrani A, Belaiche M, Es-Smairi A, Khuili M, Al-Qaisi S, Vu T V and Rai D P 2021 Electronic, magnetic, optical and transport properties of wurtzite-GaN doped with rare Earth (RE = Pm, Sm, and Eu): first principles approach *J. Surf. Interfac.* **24** 101051
[52] Mendoza-Estrada V, Gonzalez-Garcia A, Lopez-Perez W, Pinilla C and Gonzalez-Hernandez R 2017 Structural, electronic and magnetic properties of Ti-doped polar and nonpolar GaN surfaces *J. Cryst. Growth* **467** 12–7
[53] Miguel J, Espitia R, Octavio Salcedo P and López C O 2018 Electronic and magnetic behavior of transition metal-doped cubic gallium nitride: first-principles calculations *J.Magn. Magn. Mater.* **451** 295–9
[54] Xiong Z, Shi S and Jiang F 2007 Ti in GaN: Ordering ferromagnetically from first-principles study *Chem. Phys. Lett.* **443** 92–4
[55] Tran F and Blaha P 2009 Accurate band gaps of semiconductors and insulators with a semilocal exchange-correlation potential *Phys. Rev. Lett.* **102** 226401
[56] Lany S and Zunger A 2010 Dual nature of acceptors in GaN and ZnO: the curious case of the shallow Mg Ga deep state *Appl. Phys. Lett.* **96** 142114
[57] Jacobs B, Ayers V M, Petkov M P, Halpern J B, He M, Baczewski A D, McElroy K, Crimp M A, Zhang J and Shaw H C 2007 Electronic and structural characteristics of zinc-blende wurtzite biphasic homostructure GaN nanowires *Nano Lett.* **7** 1435–8
[58] Araujo R B, de Almeida J S and Ferreira Da Silva A 2013 Electronic properties of III-nitride semiconductors: a first-principles investigation using the Tran-Blaha modified Becke-Johnson potential *J. Appl. Phys.* **114** 183702
[59] Ben Sedrine N, Bouhafs C, Harmand J C, Chtourou R and Darakchieva V 2010 Effect of nitrogen on the $GaAs_{0.9-x}N_x Sb_{0.1}$ dielectric function from the near-infrared to the ultraviolet *Appl. Phys. Lett.* **97** 201903
[60] Ben Sedrine N, Rihani J, Stehle J L, Harmand J C and Chtoourou R 2008 Spectroscopic ellipsometry analysis of $GaAs_{1-x}N_x$ layers grown by molecular beam epitaxy *Mater. Sci. Eng. C* **28** 640–4
[61] Akinlami J O and Olateju I O 2015 Investigation of complex index of refraction of gallium nitride GaN *J. Nat. Sci. Eng. Technol.* **14** 29–39
[62] Muth J F, Lee J H, Shmagin I K, Kolbas R M, Cesay H C Jr, Keller B P, Mishra U K and Denbaars S P 1997 Absorption coefficient, energy gap, exciton binding energy, and recombination lifetime of GaN obtained from transmission measurements *Appl. Phys. Lett.* **71** 2572–4
[63] Indrijith Naik E, Bhojya Naik H S, Viswanath R, Kirthan B R and Prabhakara M C 2020 Effect of zirconium doping on the structural, optical, electrochemical and antibacterial properties of ZnO nanoparticles prepared by sol-gel method *Chem. Data Collect.* **29** 100505
[64] Narasimman V, Nagarrthinam V S, Usharani K and Balu A R 2017 Optoelectronic, magnetic and antibacterial properties of Zr-doped CdS thin films *Optik* **138** 398–406
[65] Li Y, Giles A and Stokes Edward B 2011 Thermal stability studies of CdSSe/ZnS quantum Dots in GaN/quantum Dots/GaN wafer bonded system *J. Electrochem. Soc.* **158** K145
[66] Khan M J I, Kanwal Z and Usmani M N 2018 Shift in optical properties of Mn doped CdS (A DFT + U study) *Mater. Res. Express* **5** 015915
[67] Azam S *et al* 2020 Effect of Fe doping on optoelectronic properties of CdS nanostructure: Insights from DFT calculations *Phys. Rev. B: Condens. Matter* **583** 412056
[68] Du Y, Chang B, Fu X, Wang X and Wang M 2012 Electronic structure and optical properties of zinc-blende GaN *Optik* **123** 2208–12
[69] Li Q, Zhu L, Li Y, Zhang X, Niu W, Guo Y and Ye Z 2017 Highly conductive thin films of nonmetal F and B co-doped ZnO on flexible substrates: Experiment and first-principles calculations *J. Alloys Compd.* **697** 156–60
[70] Li P, Deng S H, Zhang L, Li Y B, Zhang X Y and Xu J R 2010 First-principle studies on the conductive behaviors of Ga, N single-doped and Ga–N codoped ZnO *Comput. Mater. Sci.* **50** 153–7
[71] Ashokkumar M and Muthukumaran S 2015 Electrical, dielectric, photoluminescence and magnetic properties of ZnO nanoparticles co-doped with Co and Cu *J. Magn. Magn. Mater.* **374** 61–6
[72] Muhammad Ahsan H, Lal K, Saleem M, Mustafa G M and Ahamd Khan M 2021 Tuning the dielectric behavior and energy storage properties of Mn/Co co-doped ZnO *Mater. Sci. Semicond. Process.* **134** 105977